Available online at www.sciencedirect.com

ScienceDirect

Nuclear Physics A 996 (2020) 121698

NUCLEAR PHYSICS A

www.elsevier.com/locate/nuclphysa

Study of the N* momentum distribution for experimental η-mesic ^{3}He searches

N.G. Kelkar [a,*], D. Bedoya Fierro [a], H. Kamada [b], M. Skurzok [c,d]

[a] *Dept. de Fisica, Universidad de los Andes, Cra.1E No.18A-10, Santafe de Bogotá, Colombia*
[b] *Department of Physics, Faculty of Engineering, Kyushu Institute of Technology, Kitakyushu 804-8550, Japan*
[c] *INFN, Laboratori Nazionali di Frascati, Via E. Fermi, 40, 00044 Frascati (Roma), Italy*
[d] *Institute of Physics, Jagiellonian University, prof. Stanisława Łojasiewicza 11, 30-348 Kraków, Poland*

Received 30 July 2019; received in revised form 6 December 2019; accepted 13 January 2020
Available online 17 January 2020

Abstract

The proximity of the η N threshold to the mass of the N*(1535) allows us to consider the η-nucleus interaction below the η threshold as a series of excitations, decays of the N* on the constituent nucleons and the eventual decay of the N* to a nucleon and a pion. Experimental searches for η-mesic nuclei rely on this model in their analysis of data where an η-mesic nucleus could have been formed. However, the momentum distribution of an N* is often approximated to be the same as that of a nucleon inside the nucleus. Our aim is to obtain an estimate of the error introduced by this assumption and hence we calculate the momentum distribution of the N* formed inside ^{3}He. This distribution is found to be narrower than that of a nucleon inside ^{3}He. The latter affects the outgoing particles kinematics and reduces the determined acceptance of their experimental registration by the detection setup. This reduction is crucial for the determination of cross sections in the search for η-mesic helium.

Keywords: N* resonance; Momentum distribution; Search for eta mesic nuclei

* Corresponding author.
E-mail addresses: nkelkar@uniandes.edu.co (N.G. Kelkar), da.bedoya52@uniandes.edu.co (D. Bedoya Fierro), kamada@mns.kyutech.ac.jp (H. Kamada), magdalena.skurzok@lnf.infn.it (M. Skurzok).

https://doi.org/10.1016/j.nuclphysa.2020.121698
0375-9474/

1. Introduction

The S11 nucleon resonance N*(1535) has always been considered an important ingredient in the search for η-mesic nuclei. Experimental analyses for the formation of an η-mesic nucleus [1–3] often assume the η-nucleon interaction to proceed via the formation of an N* resonance as an intermediate state. For example, the analysis in [2] for the search of an η-mesic ^{4}He is carried out by assuming the reaction to proceed as $d\,d \rightarrow (^4\text{He-}\eta)_{bound} \rightarrow (\text{N}^*\text{-}^3\text{He}) \rightarrow {}^3\text{He N}\,\pi$. Therefore, for such a reaction below the η meson production threshold, an off-shell η meson produced in a $d\,d$ collision, is regarded to be absorbed on one of the nucleons in the helium nucleus and may propagate inside the nucleus by consecutive excitations and decays of the N* to a nucleon and η (off-shell) until it finally decays into an on-shell pion and a nucleon. In view of this scenario assumed in the experimental analyses, the motion of the N* in ^{4}He was analysed in [4,5]. In the analysis of the proton-deuteron fusion data in the search for η-mesic ^{3}He [6,7], the momentum distribution of the N* inside ^{3}He is necessary to establish the detector system acceptance for the registration of the $p\,d \rightarrow (d - N^*) \rightarrow d\,N\,\pi$ reaction and to determine the data selection criteria. In the absence of any theoretical calculation of the momentum distribution of the N* in ^{3}He, the experimental analyses are carried out by approximating the latter by the momentum distribution of a nucleon in ^{3}He.

The aim of the present work is to calculate the momentum distribution of the N* formed inside ^{3}He and estimate the uncertainty introduced in the experimental analysis based on approximating the former by the momentum distribution of a nucleon in ^{3}He. In order to perform such a calculation, we construct an N*-deuteron (N*-d) potential in coordinate space and solve the Schrödinger equation numerically to obtain the N*-d bound state wave functions and thereby the relative momentum distribution of the N* and the deuteron. We note that in the past couple of years, there has been a particular interest in the search of η-mesic ^{3}He through the analysis of proton-deuteron fusion reactions [6,8,9] close to the threshold of η production. In this context, the pd$\rightarrow{}^3$Heη reaction plays an important role and has been investigated theoretically to obtain an understanding of the η-^{3}He final state interaction [10] as well as the reaction mechanisms involved [11,12]. Apart from the earlier investigations [13,14] which followed the pioneering works of Refs. [15,16], the interest in this reaction [17–19] as well as η-mesic helium states [20] seems to have revived very recently [21–23].

The ongoing analyses of the WASA collaboration [7] hold the promise to confirm the theoretical findings of the past years on the possibility of forming an η-mesic ^{3}He nucleus [24,25]. These analyses involve the investigation of several possible channels such as $pd \rightarrow pd\pi^0$, $pd \rightarrow ppp\pi^-$, $pd \rightarrow pnn\pi^+$, $pd \rightarrow {}^3\text{He}\,\gamma\gamma$ etc. The experimental analysis of the $dd \rightarrow {}^3\text{He N}\pi$ reaction [2] has already shown that approximating the N* momentum distribution by that of a nucleon can significantly change the upper limits of the cross sections. Hence, it is important to investigate the N* motion in ^{3}He before finalizing the data analysis for η-^{3}He states. In the next section, we present an approach to evaluate the N*-deuteron potential in coordinate space. Using the elementary N*N interaction with one-pion and one-eta exchange as in our previous work in [5], the N*-d potential is calculated and the N*-d relative momentum distributions for two sets of N*Nπ and N*Nη coupling constants are presented in this section. In Section 3, simulations using these momentum distributions are preformed in order to determine the acceptance of the detectors and estimate the error involved in using nucleon momentum distributions in place of those of the N*. Section 4 presents an approach to evaluate the N*-d potential with the width of the N* resonance taken into account. We summarize our findings in Section 6.

2. Comparison of the N and N* momentum distributions

To evaluate the N* momentum distribution, we begin by writing an $(N^*)^+$ - deuteron potential which is constructed by using a three body approach to the $(N^*)^+$-proton-neutron system with the proton and neutron being already bound inside the deuteron. The N*-n and N*-p interaction is written using the one - pion and -eta exchange potential as in our previous works [4,5]. In [5], results were presented for several choices of the ηN*N and πN*N coupling constants. Here we choose two sets which are able to reproduce the correct branching of the N* to the πN and ηN channels, namely, $g_{N^*\pi}$ = 1.09, Λ_π = 1300 MeV, $g_{N^*\eta}$ = 2.07 and Λ_η = 1500 MeV (which we shall refer to as Set 1) [26] and $g_{N^*\pi}$ = 1.05, Λ_π = 1300 MeV, $g_{N^*\eta}$ = 1.6 and Λ_η = 1500 MeV (referred to as Set 2) [27]. In principle, there could be additional contributions from two pion exchange (ρ meson exchange diagram) and other box diagrams. However, considering the need for an estimate of the N* momentum distribution as an input for the experimental analysis and also the fact that there is no data available to fix the N N* → N N* potentials, we leave such an undertaking for the future.

2.1. N*-deuteron potential

The *pn* interaction is contained in the deuteron wave function. The N*-d potential is constructed using standard techniques from scattering theory where we first write down the scattering amplitude to obtain the potential $V_{N^*d}(\boldsymbol{q})$ in momentum space and then evaluate its Fourier transform. This procedure of obtaining potentials in coordinate space is also common in quantum field theory [28–31].

The Hamiltonian of the quantum system consisting of an N* and a nucleus (with A nucleons) is given as [32], $H = H_0 + V_{N^*A} + H_A$, where H_0 is the N*-nucleus kinetic energy operator (free Hamiltonian), $V_{N^*A} = \sum_{i=1}^{A} V_i$, the sum of N*-nucleon potentials, $V_i \equiv V_{N^*N}(|\boldsymbol{R} - \boldsymbol{r}_i|)$, where $\boldsymbol{R}$ and $\boldsymbol{r}_i$ are the coordinates of the N* and the ith nucleon with respect to the centre of mass of the nucleus and H_A is the total Hamiltonian of the nucleus containing the potential term, $\sum_{i\neq j} V_{NN}(|\boldsymbol{r}_i - \boldsymbol{r}_j|)$. We proceed with the assumption that the nucleus remains in its ground state during the scattering process, i.e., $H_A\,|\Phi\rangle = \epsilon\,|\Phi\rangle$ and that the nucleons occupy fixed positions inside the nucleus. The N* - nucleus elastic scattering amplitude can be expressed as [32]

$$f(\boldsymbol{k}', \boldsymbol{k}; E) = -(\mu/\pi)\,\langle \boldsymbol{k}', \Phi\,|\,T(E)\,|\boldsymbol{k}, \Phi\,\rangle \tag{1}$$

in terms of the matrix elements of the operator T obeying the Lippmann-Schwinger (L-S) equation, $T = V + V(E - H_0 - H_A)^{-1}T$. $|\boldsymbol{k}, \Phi\,\rangle$ and $|\boldsymbol{k}', \Phi\rangle$ are the initial and final asymptotic states which differ only in the direction of the relative N* nucleus momenta $\boldsymbol{k}$ and $\boldsymbol{k}'$. Truncating the L-S equation at first order and approximating $T = V = \sum_i V_i$, we get, $T(\boldsymbol{k}', \boldsymbol{k}) = V(\boldsymbol{k}', \boldsymbol{k})$ and denoting, $T(\boldsymbol{k}', \boldsymbol{k}) \equiv \langle \boldsymbol{k}', \Phi\,|\,T(E)\,|\boldsymbol{k}, \Phi\,\rangle$, we have

$$V(\boldsymbol{k}', \boldsymbol{k}) = \langle \boldsymbol{k}', \Phi\,|\sum_{i=1}^{A} V_i\,|\boldsymbol{k}, \Phi\,\rangle. \tag{2}$$

If the internal Jacobi coordinates are denoted by $\boldsymbol{x}_i$, then relating them with $\boldsymbol{r}_i = a_i\boldsymbol{x}_1 + b_i\boldsymbol{x}_2 + \ldots + g_i\boldsymbol{x}_{A-1}$, we can write,

$$V(\boldsymbol{k}', \boldsymbol{k}) = \int d\boldsymbol{x}_1\, d\boldsymbol{x}_2 \ldots d\boldsymbol{x}_{A-1}\,|\Phi(\boldsymbol{x}_1, \boldsymbol{x}_2, \ldots)|^2 \sum_{i=1}^{A} V_i(\boldsymbol{k}', \boldsymbol{k}, \boldsymbol{r}_i)\,, \tag{3}$$

where,

$$V_i(\boldsymbol{k}', \boldsymbol{k}, \boldsymbol{r}_i) = V_i(\boldsymbol{k}', \boldsymbol{k}) \exp[i(\boldsymbol{k} - \boldsymbol{k}') \cdot \boldsymbol{r}_i] \,. \tag{4}$$

The above discussion is valid for any nucleus with A nucleons. In case of the N*-deuteron system, Eq. (3) reduces to

$$V(\boldsymbol{k}', \boldsymbol{k}) = \int d\boldsymbol{x}_1 \, |\Phi_d(\boldsymbol{x}_1)|^2 \, [\, V_{N^*p}(\boldsymbol{k}', \boldsymbol{k}, \frac{1}{2}\boldsymbol{x}_1) + V_{N^*n}(\boldsymbol{k}', \boldsymbol{k}, -\frac{1}{2}\boldsymbol{x}_1) \,] \tag{5}$$

where we used, $\boldsymbol{x}_1 = \boldsymbol{r}_1 - \boldsymbol{r}_2$, $\boldsymbol{r}_1 = (1/2)\boldsymbol{x}_1$ and $\boldsymbol{r}_2 = -(1/2)\boldsymbol{x}_1$. We identify 1 and 2 with proton and neutron so that, $V_1 = V_{N^*p}$, $V_2 = V_{N^*n}$ and Φ_d is the deuteron wave function. Since the N*-N potentials depend only on $\boldsymbol{q}^2$, we can write, $V_{N^*N}(\boldsymbol{k}, \boldsymbol{k}') \equiv V_{N^*N}(\boldsymbol{q})$, where, $\boldsymbol{q} = \boldsymbol{k} - \boldsymbol{k}'$ is the momentum transfer carried by the exchanged pion or η meson. Denoting $Q = |\boldsymbol{q}|$, we obtain the N*-deuteron potential,

$$V_{N^*d}(Q) = \int |\Phi_d(\boldsymbol{x}_1)|^2 \left[V_{N^*p}(Q)\, e^{i\boldsymbol{q}\cdot\boldsymbol{x}_1/2} + V_{N^*n}(Q)\, e^{-i\boldsymbol{q}\cdot\boldsymbol{x}_1/2} \right] d\boldsymbol{x}_1 \,, \tag{6}$$

and hence

$$V_{N^*d}(Q) = V_{N^*p}(Q) \int d\boldsymbol{x} \, |\Phi_d(\boldsymbol{x})|^2 \, e^{-i\boldsymbol{q}\cdot\boldsymbol{x}/2} + V_{N^*n}(Q) \int d\boldsymbol{x} \, |\Phi_d(\boldsymbol{x})|^2 \, e^{i\boldsymbol{q}\cdot\boldsymbol{x}/2} \,, \tag{7}$$

in momentum space. The integrals in this expression can be shown to reduce to [33]

$$G_0(Q) = \int_0^\infty [u^2(r) + w^2(r)] \, j_0(Qr/2) \, dr \,, \tag{8}$$

where, $u(r)$ and $w(r)$ are the radial parts of the deuteron S- and D-wave functions. Thus,

$$V_{N^*-d}(Q) = (V_{N^*p}(Q) + V_{N^*n}(Q)) G_0(Q) \,, \tag{9}$$

and the Fourier transform

$$V_{N^*-d}(r) = \int e^{i\,\boldsymbol{Q}\cdot\boldsymbol{r}} \, V_{N^*-d}(Q) \, d^3Q \,, \tag{10}$$

gives the potential in coordinate space. The N*-deuteron potential in coordinate space can also be evaluated using the elementary N*-N potentials in coordinate space as

$$V_{N^*-d}(r) = \int d^3x \, |\Phi_d(\boldsymbol{x})|^2 \, V_{N^*p}(\boldsymbol{r} + \boldsymbol{x}/2) + \int d^3x \, |\Phi_d(\boldsymbol{x})|^2 \, V_{N^*n}(\boldsymbol{r} - \boldsymbol{x}/2) \,. \tag{11}$$

The explicit form of Eq. (11) will be given later in (23) for a variable N* mass, μ.

2.2. N*-deuteron momentum distribution

Using the parametrization of the Paris deuteron wave function given in [34] (with the approximation of only retaining the s-wave part), we calculate the N*-d potential in r-space and solve the Schrödinger equation numerically to find the bound states of the $(N^*)^+$-deuteron. With the coupling constants given by Set 1 mentioned in the previous section, we obtain a binding energy of -0.74 MeV and -0.33 MeV with Set 2. Evaluating the Fourier transform of the N*-d wave function obtained in r-space, we can find the relative momentum distribution of N*-d as,

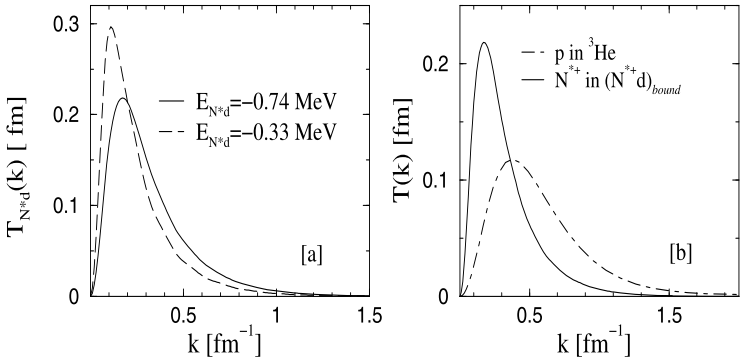

Fig. 1. Relative momentum distribution for [a] a bound system of an N* and a deuteron for two different choices of the coupling constants and [b] comparison of the N*-d momentum distribution with that of the proton in ^{3}He.

$$T(k)_{N^*d} = \frac{1}{4\pi} |\chi(k)|^2 k^2 , \tag{12}$$

where $\chi(k)$ is the bound wave function in momentum space. The above $T(k)$ is normalized as, $4\pi \int_0^\infty T(k)_{N^*d}\, dk = 1$.

In Fig. 1 we show the N*-deuteron relative momentum distribution obtained within the above approach and display it for two different sets of coupling constants in the left panel. In the right panel, we compare the N*-d momentum distribution with that of a proton in ^{3}He and find it to be narrower. This happens due to the fact that the N* binding energy is much smaller than the separation energy of a proton in ^{3}He which is ∼5.5 MeV. The wave function of the loosely bound N* is much more spread out in coordinate space and hence its Fourier transform displays a narrower distribution.

3. Relevance of N* dynamics for data analysis

As mentioned in the introduction, the important role of the N* momentum distribution in the data analysis dedicated to the search of η mesic nuclei became evident from a recent analysis of the $dd \to {}^3\mathrm{He}N\pi$ reactions [2,35]. Since no clear evidence for the existence of a narrow η-^{4}He was found in [2], upper limits of the total cross sections for the bound state production and decay in $dd \to ({}^4\mathrm{He} - \eta)_{bound} \to {}^3\mathrm{He\ n}\ \pi^0$ and $dd \to ({}^4\mathrm{He} - \eta)_{bound} \to {}^3\mathrm{He\ p}\ \pi^-$ were reported. The latter were found to change from 3 nb to 5 nb and 6 nb to 10 nb in the $\mathrm{n}\pi^0$ and $\mathrm{p}\pi^-$ channels respectively, if, the nucleon momentum distribution was replaced by that of an N* inside ^{4}He. In view of these results, the momentum distributions obtained in the present work should prove useful in the ongoing analyses of the proton-deuteron collisions to find an η-mesic ^{3}He nucleus.

In order to study the relevance of the N* momentum distribution in the search for η-^{3}He, we now apply a similar model as in [2], where, in a proton-deuteron collision, the formation of an η-^{3}He state proceeds through the repeated excitation and decay of an N*. Applying the above model, we perform Monte Carlo simulations of η-mesic bound state production and decay for beam momenta generated with a uniform probability density distribution in the range which corresponds to the experimental beam ramping and under the assumption that the bound state has a Breit-Wigner resonance structure with a fixed binding energy and width. It is further assumed that the N* in the center of mass frame displays a Fermi motion and its momentum, $\vec{k}$, is distributed isotropically with a distribution as in the present work. The deuteron four momentum

vector in the center of mass is then calculated within a spectator model assumption. The momentum vectors of the outgoing pion and nucleon emerging from the N* decay are simulated isotropically in the N* rest frame, while the absolute values of their momenta are determined knowing the N* resonance mass which is deduced using the beam momentum and the N* Fermi momentum values as

$$m_{N^*} = \left(s_{pd} + m_d^2 - 2\sqrt{s_{pd}}\sqrt{m_d^2 + |\vec{k}|^2} \right)^{1/2},$$

where s_{pd} is the energy available in the centre of mass and m_d is the mass of the deuteron. We must note here that the momentum distribution of the N* is not very sensitive to the mass of the N* itself (see the discussion in Section 3.1 in [5], Ref. [36] and references therein) and the above procedure of deducing the N* mass seems justified.

The momentum distribution of the N* inside the nucleus affects the outgoing particles kinematics (their angles and momenta) and as a consequence influences the value of the determined acceptance of their registration by the detection setup (the probability of going into the blind detection region depends on the angular distribution of the projectiles). In case of the $(^3\text{He-}\eta)_{bound}$ production in proton-deuteron collision, simulations of $pd \rightarrow (^3\text{He-}\eta)_{bound} \rightarrow \text{N}^*\text{-d} \rightarrow dp\pi^0$ performed with the N* momentum distribution presented in Fig. 1 (left panel, dashed line) result in about 60% lower geometrical acceptance of simultaneous registration of all outgoing particles in the WASA detector in comparison to those using the proton momentum distribution inside ^{3}He (right panel, dashed line). It is caused by the fact that the N*-d distribution is peaked at lower momentum values with respect to the distribution of a proton in ^{3}He. This leads to a lower acceptance as more deuterons fly inside the beam pipe and do not get detected in the forward part of the detector. The estimation was performed assuming that the angular acceptance of the detector ranges from 3° to 18° and from 20° to 169° [37]. The determined acceptance influences the cross section determination which is crucial in the analysis. The effect is even larger in the case of the low acceptance detectors, as it was for example in the case of the search for the mesic nuclei with the COSY-11 facility [38].

4. Resonance characteristics of the N*

The theoretical calculations presented in Section 2 do not take into account the fact that the N* is a broad resonance with a Breit-Wigner mass of 1535 MeV and a width of about 150 MeV. There exist different points of view on the internal structure of the N* (see [39] and references therein). We shall not enter into this discussion here since the objective of the present work is to provide a method to calculate the momentum distribution of the N* inside ^{3}He which is an essential ingredient to determine the geometrical acceptance in the experimental analysis. In order to include the resonance characteristics, we begin first by modifying the elementary N* N interaction used in this work.

4.1. Modified N N potential*

In the derivation of the N* N potential used in Section 2, the mass difference of the N* and a nucleon was neglected and hence the energy transfer in the N* N → N N* process was approximated to be zero. In what follows, we introduce a finite energy transfer at the N N* π and N N* η vertices (see Fig. 2) with the result that the N N* potential depends on the mass of the N*. The N*-d potential in coordinate space is evaluated using this N*N interaction in a similar way as in

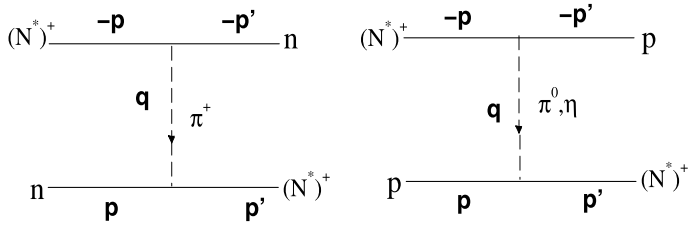

Fig. 2. Elementary N N* → N N* processes considered in this work.

Section 2. Folding the mass dependent potential with the mass distribution of the N* resonance which has a central value of 1535 MeV and width of 150 MeV, we shall obtain an effective N*-d potential which becomes mass independent and carries the information of the width of the resonance.

The one-meson exchange N N* potential was written in Ref. [5] as

$$v_x(q) = \frac{g^2_{xNN^*}}{q^2 - m_x^2}\left(\frac{\Lambda_x^2 - m_x^2}{\Lambda_x^2 - q^2}\right)^2, \tag{13}$$

with $x = \pi, \eta$ and $q^2 = \omega^2 - \mathbf{Q^2}$, the four-momentum carried by the exchanged pion or eta meson. Ref. [5] approximated $\omega = 0$ leading to

$$v_x(Q) = -\frac{g^2_{xNN^*}}{Q^2 + m_x^2}\left(\frac{\Lambda_x^2 - m_x^2}{\Lambda_x^2 + Q^2}\right)^2. \tag{14}$$

If instead we retain a finite ω and approximate it by the mass difference of the N* and the nucleon, i.e., $\omega = \mu - m_N$, (with μ being the N* mass) we get,

$$v_x(\mu, Q) = -\frac{g^2_{xNN^*}}{Q^2 - \alpha_x^2}\left(\frac{\Lambda_x^2 - m_x^2}{\beta_x^2 + Q^2}\right)^2, \tag{15}$$

where, $\alpha_x^2 = \omega^2 - m_x^2$ and $\beta_x^2 = \Lambda_x^2 - \omega^2$. Since the N* can decay to a nucleon and a π or η, the minimum mass of the N* is $m_N + m_\pi$ and α_x^2 can be positive or negative depending on the mass of the N* and the exchanged meson and the potential in (15) may have a pole. For the values of Λ_x considered in this work, β_x^2 is always positive (for N* masses below 2.2 GeV) and the term in round brackets in (15) does not have a pole. In what follows, we consider the two cases of $\alpha_x^2 < 0$ and $\alpha_x^2 > 0$ separately.

4.1.1. $\alpha_x^2 > 0$

Using the partial fraction decomposition, we can write the denominator in (15) as

$$\frac{1}{(Q^2+\beta_x^2)^2}\frac{1}{(Q^2-\alpha_x^2)} = -\frac{1}{(\alpha_x^2+\beta_x^2)^2}\frac{1}{(\beta_x^2+Q^2)} - \frac{1}{(\alpha_x^2+\beta_x^2)}\frac{1}{(\beta_x^2+Q^2)^2} + \frac{1}{(\alpha_x^2+\beta_x^2)^2}\frac{1}{(Q^2-\alpha_x^2)} \tag{16}$$

and perform the Fourier transform

$$v_x(\mu, r) = \frac{1}{2\pi^2}\int_0^\infty Q^2 v_x(\mu, Q)\frac{\sin Qr}{Qr}\, dQ \tag{17}$$

analytically to get

$$v_x(\mu, r) = \frac{g^2_{xNN^*}(\Lambda_x^2 - m_x^2)^2}{4\pi}\left[\frac{1}{(\alpha_x^2+\beta_x^2)^2}\frac{e^{-\beta_x r}}{r} + \frac{e^{-\beta_x r}}{2\beta_x(\alpha_x^2+\beta_x^2)} - \frac{e^{i\alpha_x r}}{r(\alpha_x^2+\beta_x^2)^2}\right]. \tag{18}$$

The last term arises from the following integral:

$$\int_0^\infty \frac{Q\sin(Qr)}{Q^2-\alpha_x^2-i\epsilon}\,dQ = P.V.\int_0^\infty \frac{Q\sin(Qr)}{Q^2-\alpha_x^2}\,dQ + i\frac{\pi}{2}\sin(\alpha_x r), \tag{19}$$
$$= \frac{\pi}{2}\cos(\alpha_x r) + i\frac{\pi}{2}\sin(\alpha_x r)$$

Replacing the principal value of the above integral in Eq. (18) (in place of $e^{i\alpha_x r}$) will lead us to the real part of the N*-deuteron potential. The real N*-d potential in coordinate space, as will be seen later, can be used to look for the N*-d bound states and calculate the N*-d relative momentum distribution. The mass, μ, of the N* is considered to be variable and the μ dependent potential will eventually be folded with a mass distribution $\rho(\mu)$ in order to account for the fact that the N* is a resonance with a finite width.

4.1.2. $\alpha_x^2 < 0$

Denoting, $\alpha_x^2 = -\gamma_x^2$ with $\gamma_x^2 > 0$, leads to

$$v_x(\mu, Q) = -\frac{g^2_{xNN^*}}{Q^2+\gamma_x^2}\left(\frac{\Lambda_x^2 - m_x^2}{\beta_x^2+Q^2}\right)^2. \tag{20}$$

Using the partial expansion again to write the denominator and performing the Fourier transform analytically, we get,

$$v_x(\mu, r) = -\frac{g^2_{xNN^*}(\Lambda_x^2 - m_x^2)^2}{4\pi}\left(\frac{1}{r(\gamma_x^2-\beta_x^2)^2}[e^{-\gamma_x r} - e^{-\beta_x r}] + \frac{1}{2\beta_x(\gamma_x^2-\beta_x^2)}e^{-\beta_x r}\right). \tag{21}$$

4.2. Effective N-deuteron potential*

In terms of the elementary N*-N potentials, the folding N*-d potential in coordinate space can be written as

$$V_{N^*-d}(r) = \int d^3x\,|\Phi_d(\boldsymbol{x})|^2\,V_{N^*p}(\boldsymbol{r}+\boldsymbol{x}/2) + \int d^3x\,|\Phi_d(\boldsymbol{x})|^2\,V_{N^*n}(\boldsymbol{r}-\boldsymbol{x}/2), \tag{22}$$

where V_{N^*n} and V_{N^*p} are constructed from the potentials v_x ($x = \pi^0, \pi^+, \eta$) given above (for the processes shown in Fig. 2) and $\Phi_d(\boldsymbol{x})$ is the wave function of the deuteron. Performing the angle integration (assuming only s-waves in the deuteron for simplicity) we obtain,

$$V_{N^*-d}(\mu, r) = \frac{1}{2}\int_0^\infty dy\,|u(y)|^2\,(I_{\pi^0}(y,r) + I_\eta(y,r) + 2I_{\pi^+}(y,r)), \tag{23}$$

where, for the case, $\alpha_x^2 > 0$,

$$I_x(y,r) = \frac{g_{xNN^*}^2(\Lambda_x^2 - m_x^2)^2}{4\pi y\, r\beta_x^3(\alpha_x^2+\beta_x^2)}\left[e^{-\beta_x R_-}(\beta_x R_- + 1) - e^{-\beta_x R_+}(\beta_x R_+ + 1) + \frac{2\beta_x^2}{(\alpha_x^2+\beta_x^2)}\left(e^{-\beta_x R_-} - e^{-\beta_x R_+} - \frac{\beta_x[\sin(\alpha_x R_+) - \sin(\alpha_x R_-)]}{\alpha_x}\right)\right] \tag{24}$$

and for $\alpha_x^2 < 0$, denoting $\alpha_x^2 = -\gamma_x^2$,

$$I_x(y,r) = -\frac{g_{xNN^*}^2(\Lambda_x^2 - m_x^2)^2}{4\pi y\, r\beta_x^3(\gamma_x^2-\beta_x^2)}\left[e^{-\beta_x R_-}(\beta_x R_- + 1) - e^{-\beta_x R_+}(\beta_x R_+ + 1) - \frac{2\beta_x^2}{(\gamma_x^2-\beta_x^2)}\left(e^{-\beta_x R_-} - e^{-\beta_x R_+}\right) + \frac{2\beta_x^3}{\gamma_x(\gamma_x^2-\beta_x^2)}\left(e^{-\gamma_x R_-} - e^{-\gamma_x R_+}\right)\right] \tag{25}$$

with, $x = \pi^0, \eta$ or π^+. Here, $R_\pm = |r \pm y/2|$ and the normalization of the deuteron wave function is $\int_0^\infty |u(r)|^2 dr = 1$ ($u(r)$ is the radial s-wave part of the deuteron wave function Φ_d). In fact Eq. (23) is the explicit form of Eq. (11) given in section 2.1.

The N*-d potential thus obtained depends on the mass of the N* but not the width. In order to incorporate the width and get a mass independent potential, in the final step, we introduce an effective potential weighted by the Lorentzian mass distribution $\rho(\mu)$ of the N* and write,

$$\tilde{V}_{N^*-d}(r) = \frac{\int_{\mu_0}^{\mu_{max}} V_{N^*-d}(\mu, r)\rho(\mu)d\mu}{\int_{\mu_0}^{\mu_{max}} \rho(\mu)d\mu}, \tag{26}$$

where $\mu_0 = m_N + m_\pi$ and $\rho(\mu)$ is parameterized as in [40],

$$\rho(\mu) = \frac{\Gamma_0 m^*}{\pi[(\mu^2 - m^{*2})^2 + (m^*\Gamma(\mu))^2]} \tag{27}$$

with m^* = 1535 MeV, Γ_0 = 150 MeV, and

$$\Gamma(\mu) = \Gamma_0\left(0.5\frac{k_\eta(\mu)}{k_\eta(m^*)} + 0.4\frac{k_\pi(\mu)}{k_\pi(m^*)} + 0.1\right). \tag{28}$$

The upper limit μ_{max} in (26) should in principle be ∞, but we shall introduce a finite value in order to keep β_x^2 positive (since as mentioned before, for the parameter sets chosen here, β_x^2 remains positive until $\mu \approx 2.2$ GeV). Such a cut-off seems justified since the mass distribution diminishes rapidly and any contribution to the integral above 2.2 GeV is expected to be negligible. The coefficients 0.5, 0.4 and 0.1 are the branching ratios of the N* to the η N, π N and $\pi\pi$ N channels and $k_x(\mu)$ are the momenta of the particle $x = \pi$ or η in nucleon-meson centre of mass system.

Taking the Paris parameterization [34] for the deuteron wave function and evaluating the N*-deuteron potential obtained above, we find that it does not admit any bound states for any of the N*Nπ and N*Nη coupling constants given in literature [5].

4.3. Experimental considerations

The analysis of the WASA data on the $pd \to {}^3\mathrm{He}\,\pi^0$, $pd \to pd\pi^0$ and similar channels with the objective of locating an η-mesic ^{3}He nucleus is being performed for near threshold energies. Given the range of energies for which the data is analysed, the mass of an intermediate

on-shell N* in the above process can range between 1416 to 1516 MeV. In this case, it could make some sense to limit the integration in (26) to 1516 MeV rather than considering the full range of the mass distribution. Apart from this, due to the proximity of the η N threshold to the mass of the N*, the η-nucleus interaction (forming an η-mesic nucleus) is considered to be a series of excitations and decays of the N* on the constituent nucleons until it eventually decays to a nucleon and a pion. For the sub-threshold energies at which the data is analysed, the η meson cannot be produced on-shell. However, the beam energies are way beyond the pion production threshold and therefore, once the N* decays to a pion, it is expected to be produced on-shell and leave the nucleus. In view of such a picture, we could further investigate the case of an N*-deuteron potential retaining only the η exchange diagram in the elementary N N* $\rightarrow$ N N* process.

Imposing the above conditions based on experimental considerations leads to very loosely bound states of the N* and the deuteron, bound by few tens of keV (depending on the coupling constants used). Though such an artificial cut-off in the integral over mass as well as the dropping of the pion exchange diagram is not justified in general, given the way in which the existence of an η-mesic ^{3}He is analysed, it does provide a clue for the experimental analysis that if the N* is bound, it will be very loosely bound and lead once again to a narrower momentum distribution than that of a nucleon inside ^{3}He.

5. N*-nucleus and η-nucleus bound states

As mentioned in the previous sections, the search for η-mesic bound states involves the analysis of reactions where an off-shell η meson is formed inside the nucleus. The η meson is assumed to be absorbed on a nucleon and may propagate inside the nucleus by consecutive excitations and decays of the N* to a nucleon and η (off-shell) until it finally decays into an on-shell pion and nucleon. Thus, in principle, within this description, as long as the η-mesic state exists, the N* also exists inside the nucleus. It is then natural to ask if the existence of an η-mesic bound state [41–43] necessarily implies the existence of an unstable N*-nucleus bound state. The answer to such a question is not quite straightforward. Indeed, it depends on how the N* was formed inside the nucleus. Apart from this, as shown in literature [44–46], the attractive nature of the η-nucleus system is due to the existence of N*(1535) and due to the level repulsion effect between ηN and N* (or η and N*-N-hole system). Hence, one would have to investigate the existence of the η-mesic nucleus and N*-nucleus at the same time with the inclusion of the ηNN channel. It would be of interest to perform such a calculation in future. As for the present work, we are not interested in how the N* was formed and if its binding with the nucleus has implications for the existence of an η-mesic nucleus. Our objective has been to find the momentum distribution of an N* which already exists inside the nucleus and forms a bound state with the nucleus.

6. Summary

A key ingredient in the experimental search for η-mesic helium near the threshold for η meson production is the momentum distribution of the S11 N*(1535) resonance inside the nucleus. If an η-mesic nucleus is formed, the N* is expected to be created by the strong η-N interaction, propagate, decay and get regenerated repeatedly by the η in the nucleus, until it decays eventually into a free pion and a nucleon. In an earlier work [5], the relative momentum distribution of N*-^{3}He was evaluated and used as an input for the analysis of the $dd \rightarrow {}^3$He N π reaction. The latter was analysed for the existence of η-mesic ^{4}He. There has been no conclusive evidence

for the existence of an η-mesic helium so far (see [47] for a short recent review), however, the extensive data analysis being carried out by the WASA collaboration [6] could bring us to a culmination point.

The data analysis is usually performed with the assumption that the N^* momentum distribution is similar to that of a nucleon inside the nucleus. In order to estimate the error introduced due to this assumption, we have studied the N^*-deuteron system within two scenarios. In the first one, we construct the N^*-d potential based on the elementary $N^*N \to N^*N$ interactions with the appropriate $N^*N\pi$ and $N^*N\eta$ couplings but with the assumption that the N^* is stable with a mass similar to that of a nucleon. The momentum distribution of an N^* (inside a bound $(N^*)^+$-d) evaluated within this scenario is narrower than that of a proton in ^{3}He. The latter results in a 60% reduction in the detector acceptance. The narrow momentum distribution is a result of the very low binding energy of the N^*-deuteron system. In the second scenario of an N^* with resonance characteristics, we construct the N^*-d potential taking into account the mass distribution and the width of the N^*. However, the N^*-d system is not found to be bound for any of the $N^*N\pi$ and $N^*N\eta$ couplings considered. Using certain ideas based on experimental conditions we find that the system is very loosely bound. Thus, in the realistic scenario of an N^* resonance, one would expect the momentum distribution of the N^* to be much narrower than that of a nucleon. It is important to consider this limitation in the experimental analysis of the proton-deuteron fusion reactions searching for the existence of an η-mesic ^{3}He.

Declaration of competing interest

The authors of the present work declare that there is no conflict of interest in relation to the article being submitted.

Acknowledgements

The authors are thankful to Prof. P. Moskal for many useful discussions. One of the authors (N.G.K.) thanks the Faculty of Science, Universidad de los Andes, Colombia for financial support through grant no. P18.160322.001-17. H. K. is thankful to the Japan Society for the Promotion of Science (JSPS) for financial support by Grant-in-Aid for Scientific Research (B) No. 16H04377. The numerical calculations were partially performed on the interactive server at RCNP, Osaka University, Japan.

References

[1] W. Krzemien, P. Moskal, M. Skurzok, Acta Phys. Pol. B 46 (2015) 757;
M. Skurzok, W. Krzemien, O. Rundel, P. Moskal, EPJ Web Conf. 117 (2016) 02005;
P. Adlarson, et al., Phys. Rev. C 87 (2013) 035204.
[2] P. Adlarson, et al., Nucl. Phys. A 959 (2017) 102.
[3] M. Skurzok, et al., Phys. Lett. B 782 (2018) 6.
[4] N.G. Kelkar, D. Bedoya Fierro, P. Moskal, Acta Phys. Pol. B 47 (2016) 299.
[5] N.G. Kelkar, Eur. Phys. J. A 52 (2016) 309.
[6] O. Rundel, et al., Acta Phys. Pol. B 48 (2017) 1807.
[7] M. Skurzok, et al., EPJ Web Conf. 181 (2018) 01014, arXiv:1712.06307, 2017.
[8] N.J. Upadhyay, K.P. Khemchandani, B.K. Jain, N.G. Kelkar, Phys. Rev. C 75 (2007) 054002.
[9] N.J. Upadhyay, B.K. Jain, K.P. Khemchandani, N.G. Kelkar, Mod. Phys. Lett. A 24 (2009) 2319.
[10] K.P. Khemchandani, N.G. Kelkar, B.K. Jain, Nucl. Phys. A 708 (2002) 312.
[11] K.P. Khemchandani, N.G. Kelkar, B.K. Jain, Phys. Rev. C 76 (2007) 069801.

[12] N.G. Kelkar, K.P. Khemchandani, N.J. Upadhyay, B.K. Jain, Rep. Prog. Phys. 76 (2013) 066301.
[13] K.P. Khemchandani, N.G. Kelkar, B.K. Jain, Phys. Rev. C 68 (2003) 064610.
[14] A.B. Santra, B.K. Jain, Phys. Rev. C 64 (2001) 025201.
[15] G. Faeldt, C. Wilkin, Nucl. Phys. A 587 (1995) 769.
[16] C. Wilkin, Phys. Rev. C 47 (1993) R938.
[17] P. Adlarson, et al., Phys. Lett. B 782 (2018) 297.
[18] Ju-Jun Xie, et al., Phys. Rev. C 95 (2017) 015202.
[19] H. Sadeghi, M. Goodarzi, Int. J. Theor. Phys. 54 (2015) 368.
[20] N.G. Kelkar, Acta Phys. Pol. B 46 (2015) 113.
[21] N. Barnea, E. Friedman, A. Gal, Nucl. Phys. A 968 (2017) 35.
[22] N. Barnea, et al., Phys. Lett. B 771 (2017) 297.
[23] A. Fix, O. Kolesnikov, arXiv:1801.09901, 2018.
[24] S. Wycech, A.M. Green, J.A. Niskanen, Phys. Rev. C 52 (1995) 544.
[25] N.G. Kelkar, Phys. Rev. Lett. 99 (2007) 210403.
[26] C.S. An, B. Saghai, Phys. Rev. C 84 (2011) 045204.
[27] E.J. Garzon, E. Oset, Phys. Rev. C 91 (2015) 025201.
[28] D. Bedoya Fierro, N.G. Kelkar, M. Nowakowski, J. High Energy Phys. 1509 (2015) 215;
N.G. Kelkar, F. Garcia Daza, M. Nowakowski, Nucl. Phys. B 864 (2012) 382.
[29] H.B.G. Casimir, P. Polder, Phys. Rev. 73 (1948) 360;
E.M. Lifschitz, JETP Lett. 2 (1956) 73;
F. Ferrer, J.A. Grifols, Phys. Lett. B 460 (1999) 371.
[30] R. Machleidt, Adv. Nucl. Phys. 19 (1989) 181;
J.D. Walecka, Theoretical Nuclear and Subnuclear Physics, second edition, World Scientific, 2004.
[31] N.G. Kelkar, D. Bedoya Fierro, Phys. Lett. B 772 (2017) 159.
[32] V.B. Belyaev, Lectures on the Theory of Few Body Systems, Springer-Verlag, Heidelberg, 1990;
S.A. Rakityansky, et al., Phys. Rev. C 53 (1996) R2043.
[33] L. Mathelitsch, H.F.K. Zingl, Nuovo Cimento 44 (1978) 81.
[34] M. Lacombe, et al., Phys. Lett. B 101 (1981) 139.
[35] M. Skurzok, Ph.D. thesis, Jagiellonian University, 2015, arXiv:1509.01385.
[36] S.D. Bass, Anthony W. Thomas, Phys. Lett. B 634 (2006) 368.
[37] H.-H. Adam, et al., WASA-at-COSY Collaboration, arXiv:nucl-ex/0411038, 2004.
[38] P. Moskal, J. Smyrski, Acta Phys. Pol. B 41 (2010) 2281.
[39] S.D. Bass, P. Moskal, Rev. Mod. Phys. 91 (2019) 015003.
[40] M. Wilhem, Ph.D. thesis, University of Bonn, 1992;
G. Fäldt, C. Wilkin, Nucl. Phys. A 587 (1995) 769;
A.B. Santra, B.K. Jain, Nucl. Phys. A 634 (1998) 309.
[41] Q. Haider, L.C. Liu, Phys. Lett. B 172 (1986) 257.
[42] L.C. Liu, Q. Haider, Phys. Rev. C 34 (1986) 1845.
[43] H.C. Chiang, E. Oset, L.C. Liu, Phys. Rev. C 44 (1991) 738.
[44] T. Waas, W. Weise, Nucl. Phys. A 625 (1997) 287.
[45] D. Jido, E.E. Kolomeitsev, H. Nagahiro, S. Hirenzaki, Nucl. Phys. A 811 (2008) 158.
[46] H. Nagahiro, D. Jido, S. Hirenzaki, Phys. Rev. C 80 (2009) 025205.
[47] H. Machner, EPJ Web Conf. 138 (2017) 01024.